

Reovirus μ 1 Structural Rearrangements That Mediate Membrane Penetration[∇]

Lan Zhang,¹ Kartik Chandran,^{2†} Max L. Nibert,² and Stephen C. Harrison^{1,3*}

Department of Molecular Medicine¹ and Howard Hughes Medical Institute,³ Children's Hospital, 320 Longwood Avenue, Boston, Massachusetts 02115, and Department of Microbiology and Molecular Genetics, Harvard Medical School, 200 Longwood Avenue, Boston, Massachusetts 02115²

Received 26 June 2006/Accepted 20 September 2006

Membrane penetration by nonenveloped reoviruses is mediated by the outer-capsid protein, μ 1 (76 kDa). Previous evidence has suggested that an autolytic cleavage in μ 1 allows the release of its N-terminally myristoylated peptide, μ 1N (4 kDa), which probably then interacts with the target-cell membrane. A substantial rearrangement of the remaining portion of μ 1, μ 1C (72 kDa), must also have occurred for μ 1N to be released, and some regions in μ 1C may make additional contacts with the membrane. We describe here a particle-free system to study conformational rearrangements of μ 1. We show that removal of the protector protein σ 3 is not sufficient to trigger rearrangement of free μ 1 trimer and that free μ 1 trimer undergoes conformational changes similar to those of particle-associated μ 1 when induced by similar conditions. The μ 1 rearrangements require separation of the μ 1 trimer head domains but not the μ 1N/C autocleavage. We have also obtained a relatively homogeneous form of the structurally rearranged μ 1 (μ 1*) in solution. It is an elongated monomer and retains substantial α -helix content. We have identified a protease-resistant \sim 23-kDa fragment of μ 1*, which contains the largely α -helical regions designated domains I and II in the conformation of μ 1 prior to rearrangement. We propose that the μ 1 conformational changes preceding membrane penetration or disruption during cell entry involve (i) separation of the β -barrel head domains in the μ 1 trimer, (ii) autolytic cleavage at the μ 1N/C junction, associated with partial unfolding of μ 1C and release of μ 1N, and (iii) refolding of the N-terminal helical domains of μ 1C, with which μ 1N was previously complexed, accompanied by dissociation of the μ 1 trimer.

Mammalian reoviruses have a multishelled architecture that segregates distinct functions into specific protein layers (20). The inner-capsid particle, or core, contains the complete viral transcription machinery. It enters the cell during infection but does not disassemble further. Rather, it transcribes, caps, and exports mRNA into the cytoplasm from each of the 10 viral double-stranded RNA genome segments. The core, approximately 700 Å in diameter, has an icosahedrally symmetric structure, based on 120 copies of a principal shell protein, λ 1, and 12 pentameric turrets of the multidomain capping enzyme λ 2 (8, 26). In virions, proteins μ 1 and σ 3, associated as heterohexamers (μ 1₃ σ 3₃), coat the outer surface of the core by forming a layer intercalated between the λ 2 turrets. The role of this outer layer is to mediate membrane penetration or disruption and to deposit cores into the cytoplasm (3, 13, 16, 19, 21, 22, 24, 25).

The initial step in reovirus penetration is proteolytic removal of σ 3 (2, 9, 21, 22, 27). The proteolysis, which primes μ 1 for its role in membrane translocation of the core, can occur either in the intestinal lumen, prior to receptor binding, or in endocytic vesicles. It yields an infectious subviral particle (ISVP). ISVPs can also be produced in vitro by treatment of virions with

chymotrypsin. A transient yet distinctive particle, designated ISVP*, appears to be an essential intermediate in the subsequent penetration process (3, 25). Its properties include release of the cell-attachment protein σ 1 (which projects from the λ 2 turrets on ISVPs), rearrangement of μ 1 into a protease-sensitive conformation, release of the N-terminal myristoylated peptide μ 1N (see below), and derepression of core-particle transcriptional activity.

Analysis of the molecular mechanism of reovirus core translocation requires an understanding of the structural details of μ 1 in the various conformations that it adopts during cell entry. The μ 1 protein itself is a 76-kDa polypeptide, myristoylated at its N terminus (24). An autolytic cleavage at some stage between viral assembly and entry creates fragments μ 1N (residues 2 to 42, plus the myristoyl group) and μ 1C (residues 43 to 708) (24). The fragments remain associated with each other and with the ISVP (15, 24). Mutations in μ 1 that prevent autocleavage also block membrane penetration (25). The crystal structure of μ 1₃ σ 3₃ shows that μ 1 is a tightly associated trimer, with the three σ 3 subunits projecting axially from its periphery (Fig. 1) (15). The central segment of each μ 1 polypeptide chain folds into a jelly-roll β -barrel; the N- and C-terminal parts of the chain fold together and associate with the corresponding parts of the other two chains to form a largely α -helical pedestal, which supports the apically clustered barrel domains (15). The myristoyl group at the N terminus of μ 1N is probably tucked into an elongated, hydrophobic pocket on a lateral face of this pedestal; the autocleavage site at the C terminus of μ 1N is buried within the pedestal interior (15, 29). It is necessary for infectivity (of cores recoated with μ 1₃ σ 3₃)

* Corresponding author. Mailing address: Children's Hospital, Enders 673, 320 Longwood Avenue, Boston, MA 02115. Phone: (617) 355-7372. Fax: (617) 730-1967. E-mail: Harrison@crystal.harvard.edu.

† Present address: Department of Medicine, Brigham and Women's Hospital and Harvard Medical School, Karp Family Research Laboratories, 1 Blackfan Circle, Boston, MA 02115.

[∇] Published ahead of print on 27 September 2006.

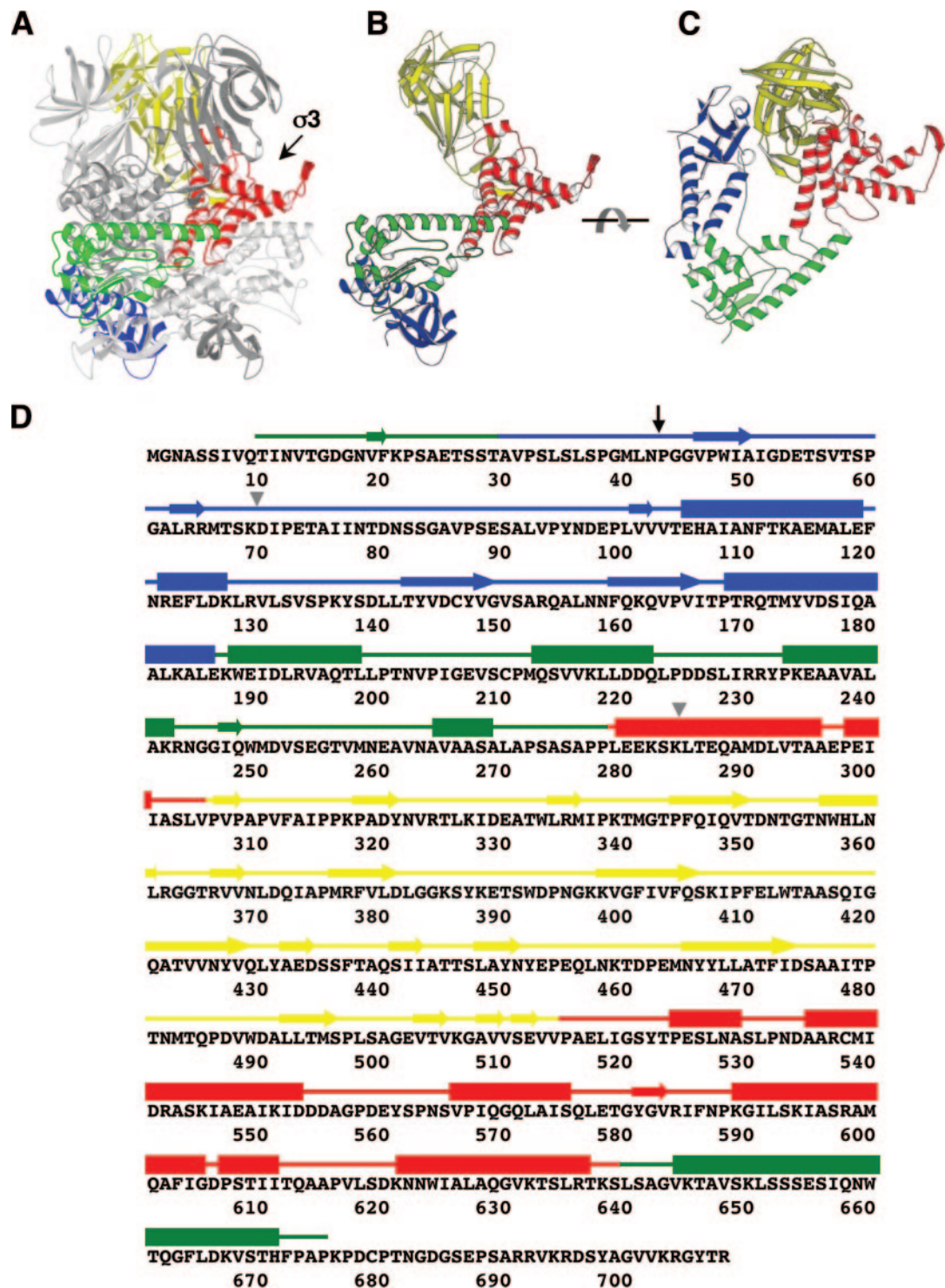


FIG. 1. $\mu 1$ prior to structural rearrangement. (A) Side view of a $\mu 1$ trimer (as in the crystal structure of the $\mu 1_3\sigma 3$ heterohexamer) without bound $\sigma 3$, with one subunit highlighted (domain I, blue; domain II, green; domain III, red; domain IV, yellow). The other two $\mu 1$ subunits are in gray. One $\sigma 3$ binding site is indicated by an arrow. (B) Side view of an isolated $\mu 1$ subunit, colored as described for panel A. (C) Top view of an isolated $\mu 1$ subunit, colored as described for panel A. (D) Amino acid sequence and secondary structure elements of reovirus $\mu 1$. The amino acid sequence of $\mu 1$ from reovirus serotype T1L is shown (5). Secondary structure elements, derived from the crystal structure of the $\mu 1_3\sigma 3$ heterohexamer (15), are presented as tubes for α -helices and arrows for β -stands. The four domains of $\mu 1$ are colored as described above. The black arrow indicates the position of the autolytic cleavage, and the gray triangles indicate the starting and ending positions of the proteolysis-resistant fragment of $\mu 1^*$.

that $\mu 1N$ is cleaved from $\mu 1C$; it is therefore plausible to suppose that productive infection requires release of $\mu 1N$ from membrane targeting through its myristoyl group, and such release of $\mu 1N$ from the ISVP* has indeed been demonstrated (25). Proximity of the three myristoyl groups and the three autocleavage sites, in the conformation of $\mu 1$ found on the virion surface as well as in the crystal structure, further suggests that cleavage, release of $\mu 1N$, and membrane targeting of $\mu 1N$ are all related events.

Inspection of the folded structure of the $\mu 1$ trimer pedestal shows that, should release of $\mu 1N$ from $\mu 1C$ indeed be a critical step, major conformational rearrangements of $\mu 1$ are likely to ensue and that these rearrangements are probably fundamental aspects of the penetration mechanism. The N-terminal segment of $\mu 1$ is tightly wound into the pedestal structure, which would have to unfold to some extent in order to release $\mu 1N$ and which might then refold into what is likely to be a very different conformation (15). This sort of reorganization underlies how the membrane fusion proteins of enveloped viruses facilitate entry (12), and it also appears to be an essential property of the rotavirus penetration protein VP4 (7). In order to determine a rearranged structure, we have established a particle-free method to promote the conformational change in $\mu 1$, by using conditions similar to those found to induce the ISVP \rightarrow ISVP* transition (3). We find that $\mu 1$ treated in this manner has properties similar to those of ISVP*-associated $\mu 1$ and that the rearrangement requires separation of the β -barrel head domains but not the $\mu 1N/C$ autocleavage. We have, moreover, obtained a relatively homogeneous form of the rearranged $\mu 1$ for biophysical characterization in solution.

MATERIALS AND METHODS

Cloning, protein expression, and purification of $\mu 1_3\sigma 3_3$ heterohexamers.

Wild-type $\mu 1_3\sigma 3_3$ heterohexamer was prepared by coexpression of the type 1 Lang (T1L) $\mu 1$ protein and $\sigma 3$ protein in insect cells infected with a recombinant baculovirus carrying the T1L M2 and S4 genes, which encode $\mu 1$ and $\sigma 3$ proteins, respectively, as previously described (5, 15). In brief, sf21 cells were grown in Hink's TNM-FH insect medium (JRH) supplemented with 10% (vol/vol) fetal bovine serum (Sigma), infected at one PFU per cell, and harvested at 72 h postinfection. The cells were resuspended by lysis buffer (20 mM Tris-Cl, pH 8.5, 2 mM $MgCl_2$, 150 mM KCl, 5 mM dithiothreitol [DTT], 2 mM benzamide, 2 $\mu g/ml$ pepstatin A, 2 $\mu g/ml$ leupeptin, and 0.2 mg/ml ethanolic phenylmethylsulfonyl fluoride [PMSF], supplemented with complete EDTA-free protease inhibitor cocktail [Roche]) at 1×10^8 cells/ml lysis buffer and disrupted by sonication on ice. Cell debris was removed by ultracentrifugation (180 kg; 1 h at 4°C). The supernatant was applied to a Q-Sepharose high-performance (HP) column (Amersham Biosciences) that was equilibrated with buffer A (20 mM Tris-Cl, pH 8.5, 2 mM $MgCl_2$, 5 mM DTT) and 150 mM NaCl. $\mu 1_3\sigma 3_3$ heterohexamer was eluted with a linear salt gradient from 150 mM to 450 mM NaCl. Then, 3 M $(NH_4)_2SO_4$ was added dropwise to the fractions containing $\mu 1_3\sigma 3_3$ to achieve a final concentration of 0.7 M. The sample was loaded onto a phenyl-Sepharose HP column (Amersham Biosciences) equilibrated in buffer A and 0.7 M $(NH_4)_2SO_4$, and eluted with a linear gradient from 0.7 M to 0 M $(NH_4)_2SO_4$. The eluted protein was diluted 1:3 with buffer A, applied to a Mono Q column (Amersham Biosciences) equilibrated with buffer A and 200 mM NaCl, and eluted with a linear salt gradient from 200 mM to 350 mM NaCl. The protein complex was further purified by gel filtration chromatography using a Superdex 200 column (Amersham Biosciences) in a buffer containing 20 mM Bicine-HCl, pH 9.0, 2 mM $MgCl_2$, 10 mM DTT, 100 mM NaCl, and 0.02% NaN_3 . The purified protein can be concentrated to 3 mg/ml and stored at $-80^\circ C$. The $(\mu 1-N42A)_3\sigma 3_3$ heterohexamer was also prepared as described above.

Amino acid changes of $\mu 1$ Ser385 \rightarrow Cys and Ser436 \rightarrow Cys for mutant DS1, as well as Thr325 \rightarrow Cys and Thr445 \rightarrow Cys for mutant DS2, were introduced into cDNA copies of the T1L M2 gene by site-directed mutagenesis using the Quick-Change method, according to the manufacturer's instructions (Stratagene).

Bsu36I-MluI restriction fragments conferring the desired mutations were subcloned into the shuttle plasmid pFastbacDUAL-M2L-S4L for recombinant baculovirus production using the Bac-to-Bac system (Invitrogen) (5, 6). The disulfide mutant $(\mu 1-DS1)_3\sigma 3_3$ and $(\mu 1-DS2)_3\sigma 3_3$ heterohexamers were purified similarly to the method described above except that DTT was absent from all the buffers.

Conformational changes of $\mu 1$ in solution. To remove $\sigma 3$ protein from $\mu 1_3\sigma 3_3$ heterohexamer, the purified wild-type or mutant protein complex (0.3 mg/ml) was incubated with various amounts of chymotrypsin in a 20- μl reaction mix containing 20 mM Tris-Cl, pH 8.5, and 100 mM NaCl or CsCl, at room temperature for 30 min. The protease digestions were quenched with the addition of 5 mM PMSF (final concentration). To trigger conformational changes in $\mu 1$, the reaction mixes were incubated at 42°C for 30 min and moved onto ice. For the trypsin sensitivity assay, the reaction mixes were divided into two parts, and one part (10 μl) was treated with trypsin at 0.1 mg/ml on ice for 1 h and quenched with the addition of 0.3 mg/ml soybean trypsin inhibitor (Worthington). The samples were disrupted by boiling for 2 to 5 min in gel loading buffer and subjected to analysis by sodium dodecyl sulfate-polyacrylamide gel electrophoresis (SDS-PAGE).

Immunoprecipitation. Monoclonal antibody (MAb) 4A3, specific for structurally rearranged $\mu 1$, was expressed and purified as described previously (28). Protein A-conjugated beads (100 μl) (Pierce) were incubated with 10 μg antibody 4A3 and 200 μl immunoprecipitation (IP) buffer (containing 10 mM Tris-Cl, pH 8.0, 150 mM NaCl, and 1% NP-40) at room temperature for 2 h and washed with 500 μl IP buffer three times. Then, 20- μl samples were added to the antibody-bound beads with 180 μl ice-cold IP buffer. The reaction mixes were incubated with rotary mixing at 4°C for 1 h and washed with 500 μl ice-cold IP buffer six times. Proteins were released from the beads by boiling in gel loading buffer for 2 to 5 min and then subjected to SDS-PAGE analysis.

Generation of recoated cores containing WT $\mu 1$ and $\mu 1-DS1$. Recoated cores containing wild-type (WT) or $\mu 1-DS1$ together with the wild-type $\sigma 3$ protein were generated from purified T1L cores and insect cell lysates containing recombinant baculovirus-expressed $\mu 1_3\sigma 3_3$ as described previously (5, 6). Recoated cores ($\mu 1-DS1$) containing Cys385-Cys436 disulfide bonds were purified from insect cell lysates by centrifugation on CsCl gradients and dialysis against virion buffer (10 mM Tris-Cl, pH 7.5, 140 mM NaCl, 1.5 mM $MgCl_2$) as described previously (5, 6). Recoated cores ($\mu 1-DS1$) lacking Cys385-Cys436 disulfide bonds were purified in a similar manner, except that CsCl gradients and dialysis buffer were supplemented to contain 40 mM β -mercaptoethanol immediately before use. Recoated cores (WT $\mu 1$) used in the experiments whose results can be seen in Fig. 3 were purified in parallel with recoated cores ($\mu 1-DS1$) as described above.

Generation of ISVP-like particles from recoated cores. Nonpurified ISVP-like particles were obtained by digesting recoated cores in virion buffer at a concentration of 5×10^{12} to 1×10^{13} particles/ml with $N\alpha$ -p-tosyl-L-lysine chloromethyl ketone-treated chymotrypsin (200 $\mu g/ml$) for 10 to 20 min at 37°C. Digestion was stopped by the addition of PMSF (2 to 5 mM) at 4°C.

Hemolysis assay. The capacities of nonpurified ISVP-like particles obtained from recoated cores to mediate hemolysis were determined as described previously (4). Briefly, washed citrated bovine calf red blood cells (RBCs; 3% [vol/vol]) were incubated with viral particles at the indicated concentrations in virion buffer containing 300 mM CsCl for 1 h at 37°C, and the extent of hemoglobin release into the supernatant was measured relative to that of controls containing only virion buffer and RBCs (0%) or water and RBCs (100%).

Purification of $\mu 1^*$. To ensure complete digestion of $\sigma 3$ and minimal cleavage of $\mu 1$, $\mu 1_3\sigma 3_3$ heterohexamer was incubated with chymotrypsin at a mass ratio of 1:4 (chymotrypsin to $\mu 1_3\sigma 3_3$ heterohexamer) in a 3-ml reaction mix containing 20 mM Tris-Cl, pH 8.5, 100 mM CsCl, and 5% foscholine-16 (Anatrace) on ice for 30 min, and protease digestion was quenched by the addition of 5 mM PMSF. Conformational rearrangement of $\mu 1$ was triggered by incubation of the reaction mix at 42°C for 30 min. The sample was immediately applied to a size exclusion column (Superdex 200; Amersham Biosciences) in a buffer containing 50 mM Bicine-HCl, pH 9.0, 10 mM DTT, 100 mM NaCl, and 0.01% foscholine-16. The purified protein can be concentrated up to 10 mg/ml and stored at $-80^\circ C$. The purified protein was analyzed by matrix-assisted laser desorption/ionization mass spectrometry (MS) and N-terminal sequencing (HHMI mass spectrometry laboratory).

Light scattering. The static light-scattering system consists of an 18-angle light-scattering detector (Dawn EOS; Wyatt Technology) in combination with a refractive index detector (Optilab Rex; Wyatt Technology). Light-scattering data were collected from about 50 μg of purified $\mu 1^*$ at room temperature using a Superdex 200 column (Amersham Biosciences) in a running buffer containing 50 mM Bicine-HCl, pH 9.0, 10 mM DTT, 100 mM NaCl, and 0.01% foscholine-16.

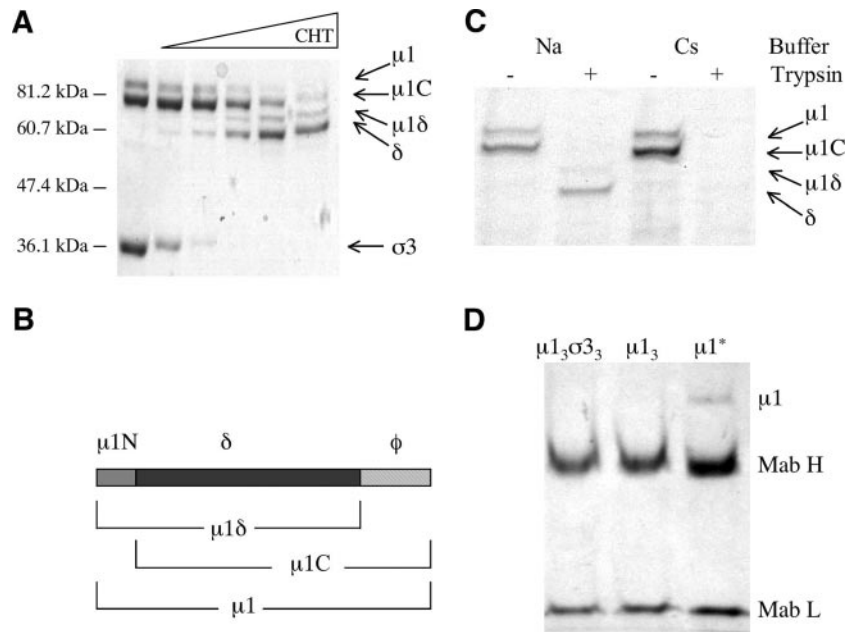


FIG. 2. Removal of $\sigma 3$ and conformational change of $\mu 1$ in solution. (A) Removal of $\sigma 3$ by digestion with chymotrypsin (CHT). The $\mu 1_3\sigma 3_3$ heterohexamer is treated with increasing amounts of chymotrypsin (first lane from left, untreated $\mu 1_3\sigma 3_3$). (B) Diagram of $\mu 1$ and its fragments. The autocleavage (between residues 42 and 43), which occurs during sample preparation, and the δ/ϕ cleavage by chymotrypsin (between residues 581 and 582) create three larger $\mu 1$ cleavage products, $\mu 1C$, $\mu 1\delta$, and δ , and two smaller fragments, $\mu 1N$ and ϕ . (C) In vitro induction of a conformational change in $\mu 1$. Free $\mu 1$ trimers, prepared as described in Materials and Methods, were incubated at 42°C for 30 min in different buffers containing either NaCl (Na) or CsCl (Cs). Each sample was treated with trypsin to detect the conformational change. (D) Structurally rearranged $\mu 1$ interacts with MAB 4A3 (28), a conformation-specific antibody. Antibody pull-down assays of wild-type $\mu 1_3\sigma 3_3$ heterohexamer, $\mu 1$ trimer ($\mu 1_3$), and rearranged $\mu 1$ ($\mu 1^*$). The bands for the heavy (H) and light (L) chains of MAB 4A3 are indicated.

Data analysis was carried out using ASTRA 5 software (Wyatt Technology) (11) after calibration and normalization with monomeric bovine serum albumin (Sigma) in the same running buffer.

CD spectrometry. The circular dichroism (CD) spectrum of purified $\mu 1^*$ at a 0.5-mg/ml concentration was measured between wavelengths of 200 and 260 nm at 25°C in a buffer containing 20 mM sodium phosphate, pH 8.0, 100 mM NaCl, 0.5 mM TCEP [Tris(2-carboxyethyl)phosphine hydrochloride], and 0.01% foscholine-16. A secondary-structure prediction program was used to estimate the amounts of different secondary-structure motifs (1). For the melting experiments, the CD spectrum of $\mu 1^*$ at wavelength 222 nm was collected from 25°C to 95°C.

Limited proteolysis. For limited proteolysis of structurally rearranged $\mu 1$, we incubated 10 μ g of purified $\mu 1^*$ with various amounts of trypsin in a 20- μ l reaction mix containing 50 mM Bicine-HCl, pH 9.0, 10 mM DTT, 100 mM NaCl, and 0.01% foscholine-16 on ice for 1 h. The reactions were quenched with the addition of 1 mg/ml soybean trypsin inhibitor and divided in two parts. One set of samples was subjected to SDS-PAGE followed by standard GelCode Blue (Pierce) staining and visual inspection. Another set of samples was applied to an SDS-PAGE gel and transferred to polyvinylidene difluoride membrane in a buffer containing 50 mM CAPS, pH 10.0, and 10% methanol (MeOH). The polyvinylidene difluoride membrane was stained with 0.025% Coomassie brilliant blue R-250 (Sigma) in 40% MeOH until samples were seen and then destained with 50% MeOH and air dried. Protein bands were cut from the dried membrane and sent for N-terminal sequencing (Tufts Core Facility). Limited proteolysis samples were also applied to matrix-assisted laser desorption ionization mass spectrometry (Tufts Core Facility).

RESULTS

Removal of $\sigma 3$ is necessary but not sufficient to trigger $\mu 1$ rearrangement in solution. To enable in vitro analysis of $\mu 1$ structural rearrangements and the ensuing membrane penetration, we sought to acquire the penetration-inducing form of $\mu 1$ (rearranged $\mu 1$, or $\mu 1^*$) free of a reovirus particle. To obtain

soluble protein from insect cells using a recombinant baculovirus vector, $\mu 1$ must be coexpressed with $\sigma 3$, and the resulting free heterohexamer ($\mu 1_3\sigma 3_3$, $\mu 1$ trimer plus three $\sigma 3$ monomers) is then stable in solution (5, 15). Although $\sigma 3$ functions as a “molecular clamp” to inhibit conformational change in the $\mu 1$ trimer (15), it appears that removal of $\sigma 3$ does not directly induce $\mu 1$ rearrangements on a virus particle but rather renders the $\mu 1$ trimers metastable, i.e., prone to undergoing conformational changes when suitably promoted (3). Interactions between adjacent $\mu 1$ trimers in the viral surface lattice, as well as those between the trimers and the viral core proteins $\lambda 2$ and $\sigma 2$ (29), may contribute to determining this metastability, and we anticipated that free $\mu 1$ trimer ($\mu 1_3$), after removal of $\sigma 3$ from free $\mu 1_3\sigma 3_3$ heterohexamer, might be unstable.

To test whether removal of $\sigma 3$ is sufficient to trigger $\mu 1$ conformational changes in solution, we expressed and purified wild-type free $\mu 1_3\sigma 3_3$ as described previously (15). Limited proteolysis by chymotrypsin led to complete digestion of $\sigma 3$ while leaving $\mu 1$ essentially intact (Fig. 2A, lanes 3 and 4). Note that two different kinds of cleavage occur in $\mu 1$, chymotryptic proteolysis in a loop between residues 581 and 582 (left exposed by the loss of $\sigma 3$), creating the fragments $\mu 1\delta$ and ϕ (Fig. 1A and D and 2B) (22), and an autocleavage between residues 42 and 43, which occurs during sample preparation for SDS-PAGE (15, 23) (Fig. 2B). We therefore observed four large $\mu 1$ fragments on the gel: intact $\mu 1$, $\mu 1C$, $\mu 1\delta$, and δ (Fig. 2A and B). The smaller fragments $\mu 1N$ and ϕ were not observed on the gel, due to its low percentage of cross-linking and an inability to resolve species with a molecular mass less than

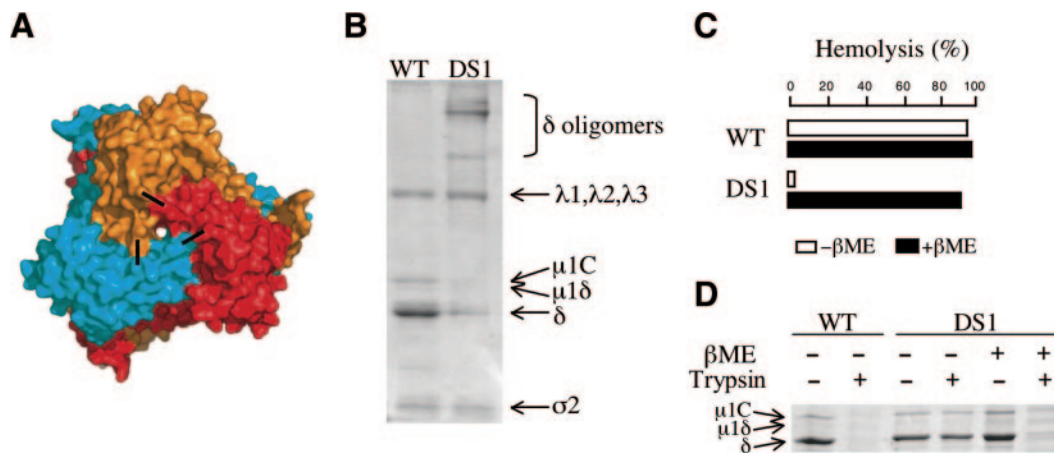


FIG. 3. An engineered interchain disulfide bond arrests $\mu 1$ conformational change and virus-induced hemolysis. (A) Surface representation of $\mu 1$ trimer, viewed from the outside relative to the orientation in virus particles. Black bars represent approximate positions of residues 385 and 436, which form an interchain disulfide bond in $\mu 1$ -DS1. (B) Disulfide bond formation in $\mu 1$ -DS1. ISVP-like particles generated by chymotryptic digestion of recoated cores and containing either wild-type $\mu 1$ ($\mu 1$ -WT) or $\mu 1$ -DS1 (5×10^{10} particles per lane) were subjected to nonreducing SDS-PAGE. Positions of viral proteins are marked. (C) Disulfide-bond-dependent arrest of hemolysis mediated by ISVP-like particles ($\mu 1$ -DS1). Recoated cores of ($\mu 1$ -WT) or ($\mu 1$ -DS1), purified in the absence or presence of 40 mM β -mercaptoethanol (β -ME), were converted to ISVP-like particles by treatment with chymotrypsin. The ISVP-like particles (5×10^{12} particles per ml) were then incubated with bovine RBCs (3% [vol/vol]) at 37°C for 20 min in the absence or presence of 40 mM β -ME. The extent of hemolysis was determined as described in Materials and Methods. (D) Status of $\mu 1$ conformational change in hemolysis reactions described for panel C. Trypsin sensitivity assays were carried out to test whether wild-type or mutant $\mu 1$ had undergone a conformational change; 10- μ l aliquots from each sample were left untreated or incubated with trypsin (100 μ g/ml) for 30 min on ice and then subjected to reducing SDS-PAGE.

about 15 kDa. Moreover, the free $\mu 1_3$ appeared to be stable *in vitro* after proteolytic removal of $\sigma 3$, as indicated by its overall insensitivity to proteolytic cleavage (Fig. 2C, lane 2) (3). The gel-filtration chromatographic profile of the $\mu 1$ trimer indicates that its three subunits remain associated with each other (L. Zhang and S. C. Harrison, unpublished data). The $\mu 1$ trimer is poorly soluble, however, and tends to aggregate over a wide range of pHs, ionic strengths, and temperatures (L. Zhang and S. C. Harrison, unpublished data). Nondenaturing detergents, such as foscholine (used in the experiments noted above whose results are unpublished to help solubilize rearranged $\mu 1$) or β -octyl glucoside, did not inhibit aggregation of the $\mu 1$ trimer (L. Zhang and S. C. Harrison, unpublished data).

A conformational change in free $\mu 1_3$ similar to one undergone by particle-associated $\mu 1_3$ in the ISVP \rightarrow ISVP* transition. One characteristic of the reovirus ISVP \rightarrow ISVP* transition is an increase in $\mu 1$ protease sensitivity, resulting from the generation of a new conformer of $\mu 1$ by structural reorganization ($\mu 1 \rightarrow \mu 1^*$) (3). $\mu 1$ trimers on the surface of reovirus T1L ISVPs undergo a conformational change at elevated temperatures (32°C and above) in the presence of K^+ , Rb^+ , or Cs^+ but not Li^+ or Na^+ ions (3, 19; K. S. Myers, M. A. Agosto, J. K. Middleton, J. Yin, and M. L. Nibert, unpublished data). To investigate whether free $\mu 1_3$ undergoes structural rearrangements under similar triggering conditions, we carried out trypsin sensitivity assays on the free trimers. Incubation of free $\mu 1_3$ in the presence of Cs^+ ions at elevated temperatures indeed yielded a protease-sensitive $\mu 1$ conformer ($\mu 1^*$) (Fig. 2C). Moreover, this species interacted with a conformation-specific MAb that recognizes rearranged $\mu 1$ on the surface of an ISVP* (3). Neither free $\mu 1_3\sigma 3_3$ nor unheated $\mu 1_3$ bound this MAb (Fig. 2D). These results suggest that the conformational change in free $\mu 1_3$ heated gently in the presence of Cs^+

ions resembles the change that $\mu 1$ undergoes on the ISVP surface when treated similarly.

The conformational changes in $\mu 1_3$ require separation of $\mu 1$ head domains. Based on analysis of the crystal structure (15), two different Cys double mutations have been introduced into $\mu 1$ at positions 385/436 ($\mu 1$ -DS1) and 325/445 ($\mu 1$ -DS2) (Fig. 1A and D and 3A). Both double mutants involve the introduction of a pair of Cys residues that can form disulfide bonds under oxidizing conditions and link adjacent β -barrel head domains (domain IV) (Fig. 3A). These $\mu 1$ disulfide-bond mutants have been used to examine whether separation of the $\mu 1$ head domains is required for the heat- and Cs^+ -induced conformational changes. ISVP-like particles derived from reovirus cores recoated with $\mu 1$ -DS1 and maintained in an oxidizing environment in which the disulfide bonds are formed (Fig. 3B) show no increase in $\mu 1$ protease sensitivity and fail to disrupt membranes, as determined by hemolysis (Fig. 3C and D). In contrast, ISVP-like particles derived from reovirus cores recoated with $\mu 1$ -DS1 and maintained in a reducing environment in which the disulfide bonds are not formed exhibit $\mu 1$ protease sensitivity and hemolysis comparable to those exhibited by ISVPs containing wild-type $\mu 1$ (Fig. 3C and D). We therefore prepared $\mu 1_3\sigma 3_3$ containing $\mu 1$ -DS1 and $\mu 1$ -DS2, using the same protocol as for wild-type heterohexamers but omitting reducing agents. Protease sensitivity assays showed that these two disulfide bonds inhibit the conformational changes in free $\mu 1_3$ (Fig. 4A), just as $\mu 1$ -DS1 inhibits the ISVP \rightarrow ISVP* transition when incorporated into $\mu 1$ on the surface of a recoated particle. The similarity of the requirements for the conformational changes in solution and on the ISVP surface supports our conclusion that $\mu 1$ undergoes the same structural transition under both circumstances.

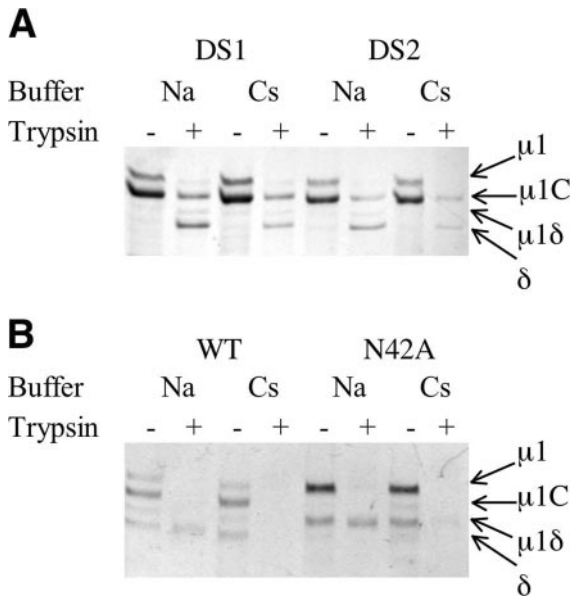


FIG. 4. Requirements for the $\mu 1$ conformational change in solution. Trypsin sensitivity assays were carried out to test whether free mutant $\mu 1$ had undergone a conformational change. Free wild-type and mutant $\mu 1$ trimers [$\mu 1_3$, ($\mu 1$ -DS1) $_3$, ($\mu 1$ -DS2) $_3$, and ($\mu 1$ -N42A) $_3$], prepared as described in Materials and Methods, were incubated at 42°C for 30 min in different buffers containing either NaCl (Na) or CsCl (Cs). Each sample was treated with trypsin to detect the conformational change. (A) The $\mu 1$ conformational change requires separation of the $\mu 1$ head domains. (B) The $\mu 1$ conformational change does not require autocleavage at the $\mu 1$ N/C junction. Note that the δ/ϕ cleavage is more extensive here than in the experiment whose results are shown in Fig. 2C, probably because of slightly different chymotrypsin to $\mu 1_3\sigma 3_3$ heterohexamers ratios.

$\mu 1$ conformational change does not require autolytic cleavage at the $\mu 1$ N/C junction. Like its wild-type counterpart, the autocleavage-inactive $\mu 1$ -N42A trimer, derived by chymotryptic removal of $\sigma 3$ from the ($\mu 1$ -N42A) $_3\sigma 3_3$ heterohexamers,

undergoes a heat- and Cs⁺-induced conformational change (Fig. 4B). This result shows that structural rearrangements in $\mu 1$ do not require autocleavage at the $\mu 1$ N/C junction. It also affords a further parallel between studies of functional properties of recoated cores and conformational properties of free $\mu 1$ trimer, as reovirus cores recoated with the ($\mu 1$ -N42A) $_3\sigma 3_3$ heterohexamers fail to enter cells but do exhibit hallmarks of the ISVP→ISVP* transition (25). The crystal structure of $\mu 1_3\sigma 3_3$ has shown that autocleavage can occur (perhaps slowly) without conformational change and even without removal of $\sigma 3$ (15). Thus, structural rearrangement and autocleavage of $\mu 1$ are not strictly dependent on each other, although the former may facilitate the latter (23).

Purification of $\mu 1^*$. Proteolytic removal of $\sigma 3$ appears to result in exposure of hydrophobic surfaces on $\mu 1$ (3). We found that the $\mu 1$ trimer aggregates over time in a variety of buffers, spanning a range of pHs and ionic strengths (L. Zhang and S. C. Harrison, unpublished). It is thus inefficient to purify $\mu 1_3$ prior to the transition to $\mu 1^*$, trigger the transition in solution, and repurify the rearranged $\mu 1$. We therefore attempted first to trigger the $\mu 1$ rearrangement without purifying $\mu 1_3$ from the limited chymotryptic digestion mixture and then to use gel-filtration chromatography to isolate $\mu 1^*$ directly. We could obtain a relatively soluble and homogeneous form of $\mu 1^*$ by using foscholine, a lipid-like detergent, to protect its hydrophobic surface. We used a minimal amount of protease to remove $\sigma 3$ so that the proteolytic cleavage site at the δ/ϕ junction of $\mu 1$ was mostly intact, triggered the $\mu 1$ conformational rearrangement in the presence of 5% foscholine (wt/vol) immediately after removal of $\sigma 3$, and recovered about one-third of the $\mu 1$ as a rearranged species by using gel-filtration chromatography to purify the product (in a buffer containing foscholine-12 or foscholine-16 at a concentration of 1.5 times its critical micelle concentration or higher). Purified $\mu 1^*$ appears to be relatively stable in detergent solution, as shown by gel-filtration chromatography after storage at 4°C for about a week (Fig. 5A). Like $\mu 1^*$ on the surface of ISVP* particles (3)

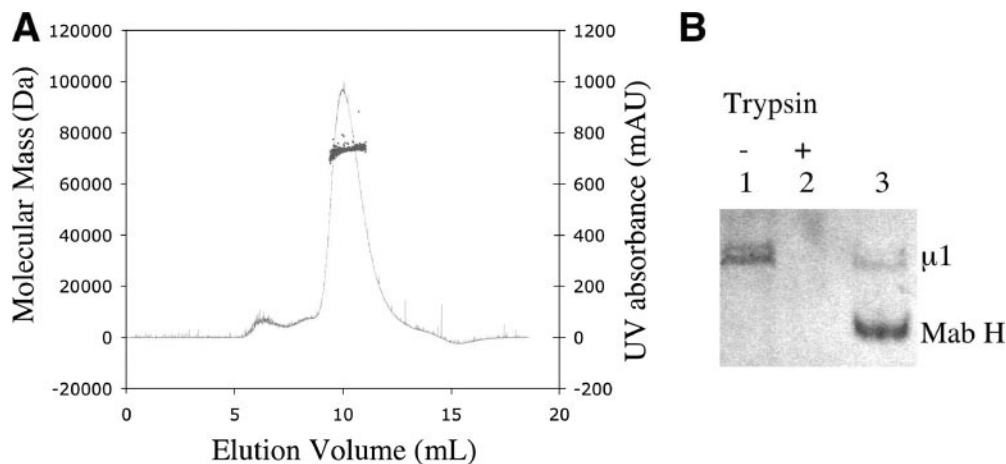


FIG. 5. Purification of rearranged $\mu 1$ ($\mu 1^*$). (A) Rearranged $\mu 1$ is a monomer in solution. Size exclusion chromatographic profile of purified $\mu 1^*$ is shown by its UV absorbance (black curve), and the estimated native molecular mass of $\mu 1^*$ calculated by the coupled static light-scattering system is also shown (gray dots). AU, absorbance units. (B) Purified $\mu 1^*$ is trypsin sensitive and interacts with a conformation-specific antibody. Lane 1 and 2, trypsin sensitivity assay of purified $\mu 1^*$. Lane 3, antibody pull-down assay of purified $\mu 1^*$. The band for the heavy chain (H) of MAb 4A3 is indicated.

and unpurified $\mu 1^*$ in solution (Fig. 2C), purified $\mu 1^*$ is protease sensitive and binds the rearrangement-specific MAb described above (Fig. 5B). These results support our conclusion that we have indeed obtained in solution a $\mu 1$ conformer that has the properties of $\mu 1^*$ on ISVP* particles. Moreover, N-terminal sequencing and mass spectrometry show that purified $\mu 1^*$ contains a polypeptide of residues 43 to 691 (Fig. 1D). These data suggest that the autocleavage has occurred at the $\mu 1N/C$ junction in purified $\mu 1^*$, and $\mu 1N$ has likely been released from purified $\mu 1^*$ (25), although our results described above show that the autocleavage is not required for the conformational rearrangement. The extreme C terminus of $\mu 1$ has also been cleaved in a disordered region (residue 691) (Fig. 1D) (15), consistent with previous findings (18, 21). It is not clear whether ϕ , if produced by chymotrypsin during $\sigma 3$ removal, still associates with the δ fragment in the rearranged conformation of $\mu 1$.

$\mu 1^*$ is a monomer in solution. We used multiangle light scattering (11) to measure the molecular mass of $\mu 1^*$ in a buffer containing 0.01% foscholine-16 (Fig. 5A). The result, 73.4 kDa, lies between the expected molecular masses of a $\mu 1$ monomer (74.4 kDa, ending at residue 691) and a $\mu 1C$ monomer (70.1 kDa, ending at residue 691). By contrast, its apparent mass estimated from the elution volume on gel-filtration chromatography is much larger, about 800 kDa (Fig. 5A). Indeed, $\mu 1^*$ elutes in an even smaller volume than the $\mu 1_3\sigma 3_3$ heterohexamer (330 kDa) in the same buffer (Zhang and Harrison, unpublished). We conclude that $\mu 1^*$ is a very elongated molecule.

$\mu 1^*$ retains substantial α -helix content. The CD spectrum of purified $\mu 1^*$ has strong negative peaks at 208 nm and 222 nm (Fig. 6A). We estimate from the CD spectrum, using the program of Andrade et al. (1), that $\mu 1^*$ contains about 21% α -helix structure and about 23% β -strand structure. In the heterohexamer, $\mu 1$ has three helical domains (I to III), with contributions from both the N- and C-terminal parts of the polypeptide chain at its base and a β -barrel domain (IV) from the middle of the chain, containing about 200 amino acids, at its apex (Fig. 1D) (15). About 27% of the $\mu 1$ residues are in α -helices, and 18% are in β -strands. Inspection of the structure suggests that the β -barrel domain is unlikely to unfold or rearrange but that the helical domains might be prone to do so. Indeed, domains I and II incorporate $\mu 1N$ in a tightly folded pattern, and the release of $\mu 1N$ would require unfolding (Fig. 1A). The percent β -strand calculated from the CD spectrum is in accord with these predictions. Moreover, a substantial fraction of α -helix present in $\mu 1$ appears to remain in $\mu 1^*$. The ratio of ellipticities at 222 nm and 208 nm can be used as an index of the presence of a coiled-coil conformation (14): the CD spectrum of $\mu 1^*$ has a $\theta_{222}/\theta_{208}$ ratio close to 0.8 (Fig. 6A), as expected for distributed helices rather than oligomeric coiled-coils. This is the anticipated result for a monomeric protein. The temperature dependence of the CD spectrum of $\mu 1^*$ (Fig. 6B) shows that the helical domains unfold at about 90°C, the temperature at which θ_{222} decreases abruptly. The helical domains are therefore very thermostable.

A stable $\mu 1^*$ fragment. We used limited proteolysis with trypsin, followed by N-terminal sequencing and MS, to identify stable fragments of $\mu 1^*$. A fragment with a molecular mass of about 23.4 kDa detected by MS extends from residue 70 to

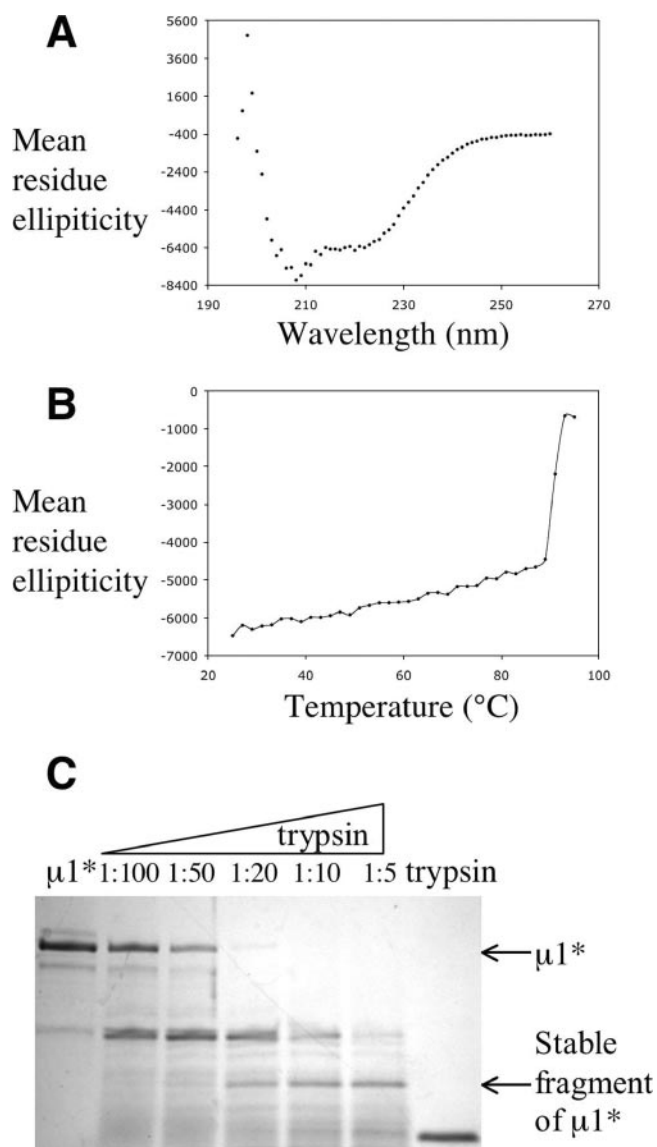


FIG. 6. Rearranged $\mu 1$ is a helical protein. (A) CD spectrum of rearranged $\mu 1$ at room temperature. (B) CD melting curve of rearranged $\mu 1$ at 222 nm. (C) Limited proteolysis of rearranged $\mu 1$. $\mu 1^*$ was treated with increasing amounts of trypsin; the mass ratio of trypsin to $\mu 1^*$ is indicated for each lane (first lane from left, untreated $\mu 1^*$; last lane from left, trypsin alone). Rearranged $\mu 1$ and a relatively stable fragment of $\mu 1^*$ are indicated by arrows.

residue 284 (Fig. 1D and 6C). Thus, it derives primarily from domains I and II (Fig. 1). The size of this stable fragment is consistent with the CD measurements, as it could account for much of the estimated α -helix content of $\mu 1^*$. Although the $\mu 1^*$ monomer is more protease sensitive than the unrearranged $\mu 1$ trimer, this fragment of $\mu 1^*$ is still relatively protease resistant, also consistent with our conclusion from the data in Fig. 6B that it has a well-ordered conformation.

DISCUSSION

In this report, we describe characteristics of the conformational rearrangements in the reovirus penetration protein, $\mu 1$.

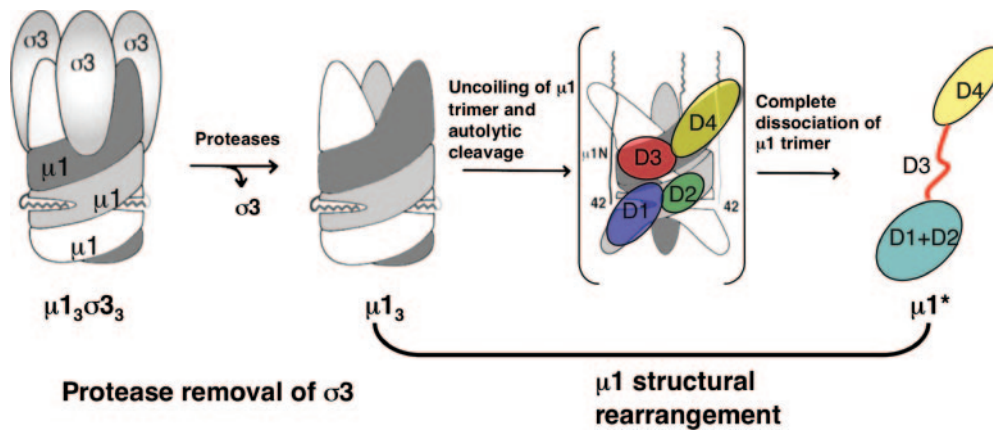


FIG. 7. Model of $\mu 1$ conformational change during reovirus entry. Proteolytic removal of $\sigma 3$ primes trimeric $\mu 1$ to undergo a conformational change in the endosome. The structural rearrangements involve uncoiling of the $\mu 1$ trimer and an autolytic cleavage, resulting in release of the N-terminally myristoylated $\mu 1N$ peptide, which can then associate with the endosomal membrane. $\mu 1C$ must unfold, at least in part, to release $\mu 1N$; it may, in the process, dissociate from the other two subunits of the trimer and refold as a monomer. Evidence in this paper suggests that the top β -barrel domain (domain IV) remains in the same conformation as in the $\mu 1_3\sigma 3_3$ heterohexamer, that the middle domain (domain III) unfolds and become flexible, and that the bottom domains, domains I and II, refold into a monomeric, largely helical structure. The color scheme for domains I to IV matches that described in the legend to Fig. 1. Note that for a clearer view of the proposed intermediate state of $\mu 1$ during the structural rearrangements, positions of domains I and II are labeled for one subunit of $\mu 1$ (in light gray) and those of domains III and IV are labeled for another subunit (in dark gray).

We demonstrate that under similar priming and promoting (or triggering) conditions, free $\mu 1$ in solution undergoes conformational changes similar to the $\mu 1$ rearrangements during the ISVP \rightarrow ISVP* transition. Removal of the $\sigma 3$ protector protein primes $\mu 1$ for structural rearrangement, i.e., proteolysis of $\sigma 3$ protein is necessary but not sufficient to trigger $\mu 1$ rearrangement in solution (Fig. 7). The metastability of the $\mu 1$ trimer after $\sigma 3$ removal (that is, its retention in the conformation present in $\mu 1_3\sigma 3_3$ until triggering) was thought to be contributed by the interactions between adjacent $\mu 1$ trimers on the virion lattice and between $\mu 1$ trimers and the viral core proteins (15). Our results suggest instead that interactions within the $\mu 1$ trimer itself contribute substantially to its metastability.

It is not clear what promotes or triggers $\mu 1$ conformational changes during infection in vivo. Exposure of reovirus ISVPs to elevated temperature in the presence of larger monovalent cations promotes the ISVP \rightarrow ISVP* transition in vitro (3). Our results confirm that under these in vitro conditions, we can produce in solution a distinct $\mu 1$ conformer ($\mu 1^*$) that mimics the structurally rearranged $\mu 1$ conformer on the ISVP* surface. A host-factor interaction by $\mu 1N$ is unlikely to be the principal trigger of the transition because the crystal structure of $\mu 1_3\sigma 3_3$ heterohexamer shows that $\mu 1N$ is tightly coiled into the base of the $\mu 1$ subunit and that its myristoyl group cannot reach to the surface of the virion without release of $\mu 1N$, i.e., without some type of conformational change having already occurred (15). Membrane interaction through some part of the $\mu 1$ protein other than the myristoylated $\mu 1N$ peptide, such as the anion binding site identified in the crystal structure of the $\mu 1_3\sigma 3_3$ heterohexamer, is another candidate for a triggering event (15). K^+ ions, which promote the ISVP \rightarrow ISVP* transition in vitro in the same way as do Cs^+ ions (3; Myers et al., unpublished), might also have a role. The $\mu 1$ structural rearrangements might also be initiated by other reovirus surface proteins in vivo. For example, binding

of $\sigma 1$ protein to the cellular receptor might induce opening of the $\lambda 2$ turret, and the conformational change of $\lambda 2$ might then propagate to $\mu 1$ (10).

The conformational transition of $\mu 1$ involves two major changes: cleavage and release of the myristoylated $\mu 1N$ peptide and substantial structural rearrangements in $\mu 1C$ (Fig. 7) (3, 15, 25). Either the released myristoylated $\mu 1N$ peptide or the structurally rearranged $\mu 1C$, or both, might be responsible for direct membrane interaction. Reovirus cores recoated with a mutant $\mu 1$ N42A protein, which cannot undergo autocleavage and which is inactive in mediating cell entry of those particles, still exhibit a number of the characteristics of the ISVP \rightarrow ISVP* transition in vitro (25). Our results with $\mu 1$ -N42A trimers confirm that the $\mu 1$ conformational change in solution does not require cleavage at the $\mu 1N/C$ junction. The $\mu 1N$ peptide cannot be released and reach the cellular membrane, however, without substantial changes in $\mu 1$ and possibly dissociation of the $\mu 1$ trimer (15). Autocleavage and $\mu 1$ conformational change are thus likely to be coupled events on the surface of the ISVP and during the infectious process. Moreover, although the crystal structure of the $\mu 1_3\sigma 3_3$ heterohexamer shows that autocleavage can occur in vitro even without proteolytic removal of $\sigma 3$ (15), recent electron microscope data suggest that the majority of the $\mu 1$ subunits on the virus surface contain an uncleaved peptide bond at the $\mu 1N/C$ junction (29). Biochemical analysis of $\mu 1$ both in solution (L. Zhang, S. C. Harrison, and M. L. Nibert, unpublished data) and on the ISVP surface (23) suggest that autocleavage takes place during the ISVP \rightarrow ISVP* transition, as part of the larger-scale structural changes. Although purified $\mu 1^*$ likely consists of a cleaved form of $\mu 1$ and previous study has suggested that the $\mu 1N$ peptide is indeed released from $\mu 1C$ during the ISVP \rightarrow ISVP* transition (25), we cannot conclude yet whether the cleaved $\mu 1N$ peptide remains associated with the rest of

the molecule in solution, due to the low resolution of the molecular mass estimation obtained by light scattering.

Our results allow us to outline some of the structural features of $\mu 1^*$, the product of the conformational changes (Fig. 7). It is a monomer in solution and exposes substantial hydrophobic surface. Mutations that cross-link the head domains of $\mu 1$ trimers inhibit the conformational changes in $\mu 1$ (Fig. 3 and 4A), and many of the known mutations in $\mu 1$ that confer enhanced thermostability on virions have mapped to subunit interfaces within a trimer (13). Both of these observations suggest that dissociation of trimer interfaces occurs during the ISVP \rightarrow ISVP* transition and not just during conformational changes in isolated $\mu 1$. The $\mu 1$ head domain, a jelly-roll β -barrel, appears likely to fold independently of the rest of the subunit and is not likely to undergo a large structural rearrangement. The amount of β -strand in $\mu 1^*$, as estimated from its CD spectrum, is consistent with this suggestion. Domains I to III of $\mu 1$ are mainly α -helical and intertwined with helical domains from other subunits of the trimer. We believe that it is these domains that refold during trimer dissociation. Moreover, these helical domains contain several hydrophobic sequences and long amphipathic helices, which might be responsible for the hydrophobicity and probable membrane interaction of $\mu 1^*$.

The hydrodynamic properties of $\mu 1^*$ suggest that the helical domains adopt a substantially more elongated structure than they do in the $\mu 1$ trimer. The total helix content of $\mu 1$ appears to decrease somewhat during the transition from $\mu 1$ to $\mu 1^*$, but a reasonable fraction remains. The stable fragment of $\mu 1^*$ produced by limited proteolysis contains most of domains I and II, and if the residues in their constituent helices remain helical, those segments could account for most of the α -helical portions of $\mu 1^*$. We therefore suggest that $\mu 1^*$ contains much of domains I and II in an elongated alignment, with a flexible (and protease-sensitive) link, created by the unfolding of domain III, to the β -barrel (Fig. 7). The long α -helix near the C terminus of $\mu 1$ contributes to domain II, anchoring the polypeptide chain within this domain upon its return from the β -barrel. It is possible that this segment, which would not have been easily detected in our analysis of limited proteolysis data, also contributes to the elongated, monomeric $\mu 1^*$. Limited proteolysis of ISVP* in the absence of membrane generates a different protease-resistant fragment of $\mu 1^*$, which contains the β -barrel domain (21); interaction between this domain and other proteins of the virus may protect it from protease cleavage. The enhanced stability of domains I and II of $\mu 1^*$ in the presence of foscholine suggests that the refolded helical portions of $\mu 1^*$ participate in membrane interaction.

The structural protein VP6 of rotavirus has an overall structure similar to that of $\mu 1$ (its conformation in the $\mu 1_3\sigma 3_3$ heterohexamer), suggesting an evolutionary relationship between these two proteins. VP6 does not, however, mediate membrane penetration. Like $\mu 1$, VP6 forms a tight trimer, but its folded structure consists of only two distinct domains: a distal β -barrel, which is analogous to domain IV of $\mu 1$, and a proximal α -helical domain, which interacts with the inner layer of the virion (17). Consistent with our data, structural comparison of $\mu 1$ and VP6 also suggests that the additional α -helical elements of $\mu 1$ at the base of the trimer, mostly from domains

I and II, might be the components that mediate the membrane-penetration function of $\mu 1$.

The penetration machineries of nonenveloped viruses undergo primed and triggered conformational rearrangements to facilitate cell entry, just as the fusion machineries of enveloped viruses do. A number of nonenveloped viruses, exemplified by reoviruses, picornaviruses, and probably polyomaviruses, have an N-terminally myristoylated peptide cleaved from or associated with a jelly-roll β -barrel subunit. Proteolytic cleavage is also a critical priming step in the case of rotavirus VP4, which has neither an N-terminal myristoyl group nor a standard jelly-roll β -barrel but does have a surface likely to associate with a lipid bilayer when exposed by the cleavage (7). It remains a puzzle whether membrane penetration by nonenveloped viruses involves a defined penetration pore or a more generalized lysis of an endosomal membrane. In the case of reovirus $\mu 1$, a higher-order oligomer of the conformationally rearranged protein has not yet been identified. We anticipate that the results described here can lead us to a strategy for obtaining a high-resolution structure of $\mu 1^*$.

ACKNOWLEDGMENTS

We thank A. L. Odegard for constructing the recombinant baculovirus carrying genes encoding the mutant ($\mu 1$ -N42A) $_3\sigma 3_3$ protein; D. S. King at the HHMI mass spectrometry laboratory and the Tufts Core Facility for mass spectrometry and N-terminal sequencing; J. Zimmer for help with the static light-scattering experiment; and members of the Harrison and Nibert laboratories for helpful discussions.

This work was supported in part by NIH grants R01 CA13202 to S.C.H. and R01 AI46440 to M.L.N. L.Z. acknowledges a Helen Hay Whitney postdoctoral fellowship, and K.C. acknowledges a Bernard N. Fields postdoctoral fellowship.

REFERENCES

1. Andrade, M. A., P. Chacon, J. J. Merelo, and F. Moran. 1993. Evaluation of secondary structure of proteins from UV circular dichroism spectra using an unsupervised learning neural network. *Protein Eng.* **6**:383–390.
2. Bodkin, D. K., M. L. Nibert, and B. N. Fields. 1989. Proteolytic digestion of reovirus in the intestinal lumens of neonatal mice. *J. Virol.* **63**:4676–4681.
3. Chandran, K., D. L. Faretta, and M. L. Nibert. 2002. Strategy for nonenveloped virus entry: a hydrophobic conformer of the reovirus membrane penetration protein $\mu 1$ mediates membrane disruption. *J. Virol.* **76**:9920–9933.
4. Chandran, K., J. S. Parker, M. Ehrlich, T. Kirchhausen, and M. L. Nibert. 2003. The delta region of outer-capsid protein $\mu 1$ undergoes conformational change and release from reovirus particles during cell entry. *J. Virol.* **77**:13361–13375.
5. Chandran, K., S. B. Walker, Y. Chen, C. M. Contreras, L. A. Schiff, T. S. Baker, and M. L. Nibert. 1999. In vitro re coating of reovirus cores with baculovirus-expressed outer-capsid proteins $\mu 1$ and $\sigma 3$. *J. Virol.* **73**:3941–3950.
6. Chandran, K., X. Zhang, N. H. Olson, S. B. Walker, J. D. Chappell, T. S. Dermody, T. S. Baker, and M. L. Nibert. 2001. Complete in vitro assembly of the reovirus outer capsid produces highly infectious particles suitable for genetic studies of the receptor-binding protein. *J. Virol.* **75**:5335–5342.
7. Dormitzer, P. R., E. B. Nason, B. V. Prasad, and S. C. Harrison. 2004. Structural rearrangements in the membrane penetration protein of a nonenveloped virus. *Nature* **430**:1053–1058.
8. Dryden, K. A., G. Wang, M. Yeager, M. L. Nibert, K. M. Coombs, D. B. Furlong, B. N. Fields, and T. S. Baker. 1993. Early steps in reovirus infection are associated with dramatic changes in supramolecular structure and protein conformation: analysis of virions and subviral particles by cryoelectron microscopy and image reconstruction. *J. Cell Biol.* **122**:1023–1041.
9. Ebert, D. H., J. Deussing, C. Peters, and T. S. Dermody. 2002. Cathepsin L and cathepsin B mediate reovirus disassembly in murine fibroblast cells. *J. Biol. Chem.* **277**:24609–24617.
10. Fernandes, J., D. Tang, G. Leone, and P. W. Lee. 1994. Binding of reovirus to receptor leads to conformational changes in viral capsid proteins that are reversible upon virus detachment. *J. Biol. Chem.* **269**:17043–17047.
11. Foltá-Stogniew, E., and K. R. Williams. 1999. Determination of molecular masses of proteins in solution: implementation of an HPLC size exclusion

- chromatography and laser light scattering service in a core laboratory. *J. Biomol. Tech.* **10**:51–63.
12. **Harrison, S. C.** 2005. Mechanism of membrane fusion by viral envelope proteins. *Adv. Virus Res.* **64**:231–261.
 13. **Hooper, J. W., and B. N. Fields.** 1996. Role of the $\mu 1$ protein in reovirus stability and capacity to cause chromium release from host cells. *J. Virol.* **70**:459–467.
 14. **Lau, S. Y., A. K. Taneja, and R. S. Hodges.** 1984. Synthesis of a model protein of defined secondary and quaternary structure. Effect of chain length on the stabilization and formation of two-stranded alpha-helical coiled-coils. *J. Biol. Chem.* **259**:13253–13261.
 15. **Liemann, S., K. Chandran, T. S. Baker, M. L. Nibert, and S. C. Harrison.** 2002. Structure of the reovirus membrane-penetration protein, $\mu 1$, in a complex with its protector protein, $\sigma 3$. *Cell* **108**:283–295.
 16. **Lucia-Jandris, P., J. W. Hooper, and B. N. Fields.** 1993. Reovirus M2 gene is associated with chromium release from mouse L cells. *J. Virol.* **67**:5339–5345.
 17. **Mathieu, M., I. Petitpas, J. Navaza, J. Lepault, E. Kohli, P. Pothier, B. V. Prasad, J. Cohen, and F. A. Rey.** 2001. Atomic structure of the major capsid protein of rotavirus: implications for the architecture of the virion. *EMBO J.* **20**:1485–1497.
 18. **Mendez, I. L., Y. M. She, W. Ens, and K. M. Coombs.** 2003. Digestion pattern of reovirus outer capsid protein $\sigma 3$ determined by mass spectrometry. *Virology* **311**:289–304.
 19. **Middleton, J. K., T. F. Severson, K. Chandran, A. L. Gillian, J. Yin, and M. L. Nibert.** 2002. Thermostability of reovirus disassembly intermediates (ISVPs) correlates with genetic, biochemical, and thermodynamic properties of major surface protein $\mu 1$. *J. Virol.* **76**:1051–1061.
 20. **Nibert, M., and L. A. Schiff.** 2001. Reoviruses and their replication, p. 1679–1728. *In* D. M. Knipe and P. M. Howley (ed.), *Fields virology*, 4th ed. Lippincott, Williams & Wilkins, Philadelphia, Pa.
 21. **Nibert, M. L.** 1989. Ph.D. thesis. Harvard University, Boston, Mass.
 22. **Nibert, M. L., and B. N. Fields.** 1992. A carboxy-terminal fragment of protein $\mu 1/\mu 1C$ is present in infectious subvirion particles of mammalian reoviruses and is proposed to have a role in penetration. *J. Virol.* **66**:6408–6418.
 23. **Nibert, M. L., A. L. Odegard, M. A. Agosto, K. Chandran, and L. A. Schiff.** 2005. Putative autocleavage of reovirus $\mu 1$ protein in concert with outer-capsid disassembly and activation for membrane permeabilization. *J. Mol. Biol.* **345**:461–474.
 24. **Nibert, M. L., L. A. Schiff, and B. N. Fields.** 1991. Mammalian reoviruses contain a myristoylated structural protein. *J. Virol.* **65**:1960–1967.
 25. **Odegard, A. L., K. Chandran, X. Zhang, J. S. Parker, T. S. Baker, and M. L. Nibert.** 2004. Putative autocleavage of outer capsid protein $\mu 1$, allowing release of myristoylated peptide $\mu 1N$ during particle uncoating, is critical for cell entry by reovirus. *J. Virol.* **78**:8732–8745.
 26. **Reinisch, K. M., M. L. Nibert, and S. C. Harrison.** 2000. Structure of the reovirus core at 3.6 Å resolution. *Nature* **404**:960–967.
 27. **Sturzenbecker, L. J., M. Nibert, D. Furlong, and B. N. Fields.** 1987. Intracellular digestion of reovirus particles requires a low pH and is an essential step in the viral infectious cycle. *J. Virol.* **61**:2351–2361.
 28. **Virgin, H. W., IV, and K. L. Tyler.** 1991. Role of immune cells in protection against and control of reovirus infection in neonatal mice. *J. Virol.* **65**:5157–5164.
 29. **Zhang, X., Y. Ji, L. Zhang, S. C. Harrison, D. C. Marinescu, M. L. Nibert, and T. S. Baker.** 2005. Features of reovirus outer capsid protein $\mu 1$ revealed by electron cryomicroscopy and image reconstruction of the virion at 7.0 angstrom resolution. *Structure (Cambridge)* **13**:1545–1557.